IEEE Photonics Journal
An IEEE Photonics Society Publication

Open Access

Bifocal Fibonacci Diffractive Lenses

Volume 5, Number 3, June 2013

J. A. Monsoriu
A. Calatayud
L. Remón
W. D. Furlan
G. Saavedra
P. Andrés

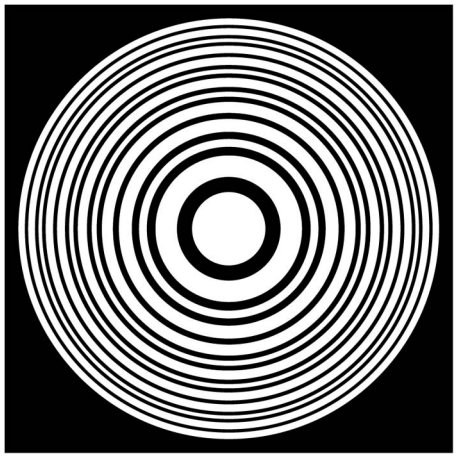

DOI: 10.1109/JPHOT.2013.2248707
1943-0655/$31.00 ©2013 IEEE

IEEE photonics SOCIETY

IEEE

Bifocal Fibonacci Diffractive Lenses

J. A. Monsoriu,[1] A. Calatayud,[1] L. Remón,[1] W. D. Furlan,[2] G. Saavedra,[2] and P. Andrés[2]

[1]Centro de Tecnologías Físicas, Universitat Politècnica de València, E-46022 Valencia, Spain
[2]Departamento de Óptica, Universitat de València, E-46100 Burjassot, Spain

DOI: 10.1109/JPHOT.2013.2248707
1943-0655/$31.00 ©2013 IEEE

Manuscript received February 13, 2013; accepted February 18, 2013. Date of publication February 22, 2013; date of current version June 20, 2013. This work was supported in part by the Ministerio de Economía y Competitividad under Grants FIS2011-23175 and TRA2009-0215, by the Generalitat Valenciana under Grant PROMETEO2009-077, and by the Universitat Politècnica de València, Spain, under Grants PAID-05-11 and SP20120569. The work of L. Remón was supported by a fellowship of "Fundación Cajamurcia," Spain. Corresponding author: J. A. Monsoriu (e-mail: jmonsori@fis.upv.es).

Abstract: The focusing properties of diffractive lenses designed using the Fibonacci sequence are studied. It is demonstrated that these lenses present two equal intensity foci and that the ratio of the two focal distances approaches the golden mean. This distinctive optical characteristic is experimentally confirmed. It is suggested that the versatility and potential scalability of these lenses may allow for new applications ranging from X-ray microscopy to THz imaging.

Index Terms: Fibonacci, diffraction, zone plates.

1. Introduction

The observation of nature has allowed scientists to perceive different kinds of morphological orders, including the Fibonacci sequence, one of the most recurrent mathematical fitting models. The ratio of two consecutive elements of the Fibonacci sequence approaches asymptotically an irrational number known as the golden mean. This number has been historically associated with the concepts of equilibrium, harmony, and even beauty. Fibonacci series and the golden mean have been ubiquitously observed in nature, from the helical arrangement of seeds and leaves (Phyllotaxis) of plants [1] to all dynamical systems exhibiting the period-doubling route to chaos [2]. Artificial Fibonacci patterns also appear on core/shell structures constructed through stress-driven self-assembly induced by cooling [3], and the golden mean has recently been found in the fine structure of spin dynamics around critical points in quantum phase transitions [4], just to name a few. Due to the rapid development of its associated technology, photonics is a potential field of applications for novel devices designed and constructed using the Fibonacci sequence. Two recent examples of significant impact are the fabrication of quantum cascade lasers based on a Fibonacci distributed feedback sequence and Fibonacci arrays of nanoparticles that produce quasi-periodic distribution of plasmon modes. Both applications have unique properties [5], [6].

In photonics technology, diffractive optical elements (DOEs) have found a large number of new applications that satisfy the increasing demand for more compact, light-weight, and cost-effective optical systems and components. In addition, a single DOE can combine various functions, providing a greater flexibility in system configuration and mounting. A wide range of applications arises mainly in areas where conventional refractive optics does not provide good solutions. DOEs are essentially bidimensional and thus not voluminous like the refractive ones. They are therefore ideal, for example, in X-ray microscopy [7], THz optics [8], and in some branches of ophthalmology [9].

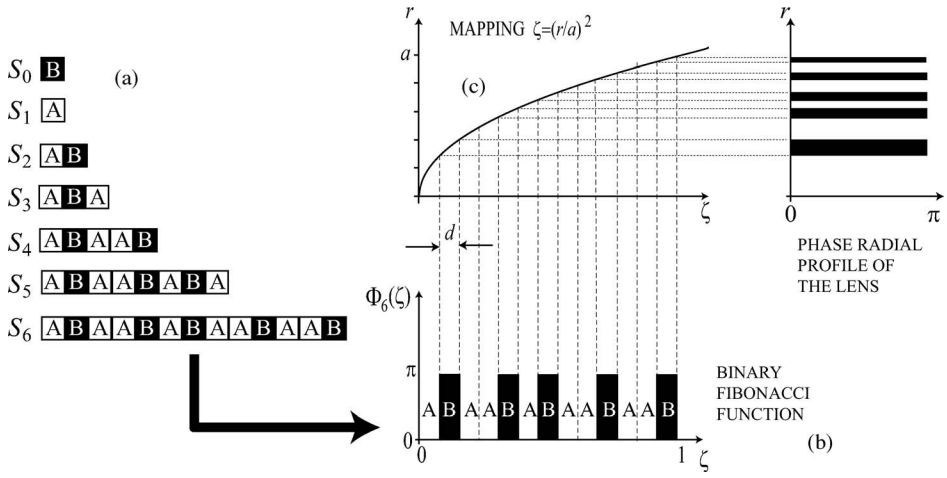

Fig. 1. (a) Generation of Fibonacci structures based on the Fibonacci sequence according to the rule $S_{j+1} = \{S_j\ S_{j-1}\}$. (b) A binary (0, π) phase function, $\Phi_j(\zeta)$ is constructed from a given Fibonacci structure (S_6 in this case). (c) A nonuniform mapping of this function gives the radial profile of the FL.

Nowadays, most diffractive lenses in use are however still conventional Fresnel zone plates, which have inherent limitations. Fractal zone plates [10], [11] are a new type of multifocal diffractive lenses that have been proposed to overcome some of these limitations. In fact, it was shown that these lenses, generated with the fractal Cantor set, have an improved behavior, especially under wideband illumination [12]. Another interesting mathematical generator of aperiodic zone plates is the Fibonacci sequence [13]. This sequence has been employed in the development of different photonic devices [14], as for example, multilayers and linear gratings [15], circular gratings [16], and spiral zone plates [17]. In this paper, we show that Fibonacci lenses (FLs) are intrinsically bifocals with the ratio of the two focal distances approaching the golden mean. This property is experimentally verified, and the results are compared with those obtained with a conventional Fresnel zone plate.

2. Fibonacci Lenses

Starting with two elements (seeds) $F_0 = 0$ and $F_1 = 1$, the Fibonacci numbers, $F_j = \{0, 1, 1, 2, 3, 5, 8, 13, 21, \ldots\}$, are obtained by the sequential application the following rule: $F_{j+1} = F_j + F_{j-1}$, $(j = 0, 1, 2, \ldots)$. The golden mean or golden ratio is defined as the limit of the ratio of two consecutive Fibonacci numbers

$$\varphi = \lim_{j\to\infty} F_j/F_{j-1} = (1 + \sqrt{5})/2. \tag{1}$$

Based on the Fibonacci numbers, a binary aperiodic Fibonacci sequence can also be generated with two seed elements shown in Fig. 1(a), as for example, $S_1 = A$ and $S_0 = B$. Then, each element of the sequence is obtained simply as the concatenation of the two previous element $S_{j+1} = \{S_j\ S_{j-1}\}$ for $j \geq 1$. Therefore, $S_2 = AB$, $S_3 = ABA$, $S_4 = ABAAB$, $S_5 = ABAABABA$, etc. In the sequence, two successive "B" are separated by either one or two "A." The total number of elements of a given sequence is F_{j+1}, which results from the sum of F_j elements "A," plus F_{j-1} elements "B." When designing an FL, each of these sequences can be used to define the binary generating function $\Phi_j(\zeta)$ with compact support on the interval [0, 1] [see Fig. 1(b)]. This interval is partitioned in F_{j+1} subintervals of length $d = 1/F_{j+1}$, and the value that takes at the kth subinterval is associated to the value of the element S_{jk}, being 0 or π when S_{jk} is "A" or "B," respectively. Mathematically, this condition is expressed in a general form as $\Phi_j(\zeta) = 0$ if $(\lfloor l\varphi \rfloor - 1)d \leq \zeta < (\lfloor l\varphi \rfloor)d$, for $l = \{1, 2, \ldots, F_j\}$, and $\Phi_j(\zeta) = \pi$ otherwise, where $\lfloor\varphi\rfloor$ denotes the largest integer less than or equal to φ.

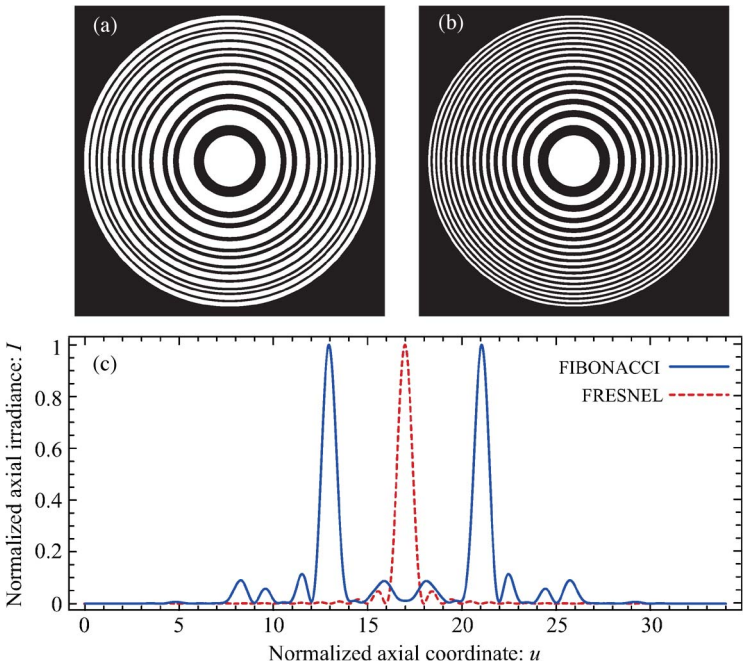

Fig. 2. (a) Fibonacci lens generated from the 1-D function $\Phi_8(\zeta)$. White and black rings correspond to a phase 0 and π, respectively. (b) Fresnel zone plate of the same resolution. (c) Numerically computed axial irradiance produced by both lenses against the normalized axial distance u.

From a particular generating function $\Phi_j(\zeta)$, the transmittance of the corresponding binary phase-only diffractive FL is obtained as $q(\zeta) = \exp[i\Phi_j(\zeta)]$, after performing the following coordinate transformation: $\zeta = (r/a)^2$, where r is the radial coordinate of the lens, and a is its maximum value [see Fig. 1(c)]. A typical diffractive FL is shown in Fig. 2(a). For comparison, a conventional Fresnel zone plate with the same resolution is represented in Fig. 2(b). Note that the Fresnel zone plate can be obtained using the same approach but by replacing the aperiodic Fibonacci structure with a periodic one (i.e., a sequence of F_{j+1} alternating white and black boxes in Fig. 1). Therefore, an FL can be understood as a conventional Fresnel zone plate with period $p = 2d$, where the positions of some zones with different phase have been interchanged. Moreover, as stated in [14], a Fibonacci sequence is aperiodic with two incommensurable periods. According to our nomenclature, in an FL, these periods are given by $p_1/p = 0.5\ F_{j+1}/F_{j-1} \approx 0.5\ (\varphi + 1)$ and $p_2/p = 0.5\ F_{j+1}/\ F_j \approx 0.5\ \varphi$. Thus, an FL can be understood as two Fresnel zone plates interlaced. The axial irradiance distribution produced by an FL and its associated Fresnel zone plate was numerically calculated using the Fresnel–Kirchhoff diffraction theory as

$$I(u) = 4\pi^2 u^2 \left| \int_0^1 q(\zeta) \exp(-i2\pi u\zeta)\, d\zeta \right|^2 \tag{2}$$

where $u = a^2/2\lambda z$ is the reduced axial coordinate, λ is the wavelength of the light, and z the axial distance from the pupil plane.

The axial irradiances, corresponding to the first-order diffraction foci, computed for an FL of order S_8 and its associated Fresnel zone plate are shown in Fig. 2(c). It can be seen that, in this case $(j = 8)$, the first focus of the FL is located at $u_1 = 13 = F_7 = F_{j-1}$ and the other one at $u_2 = 21 = F_8 = F_j$. Thus, the ratio of the focal distances satisfies $u_2/u_1 \approx \varphi$. The axial irradiance distribution, represented against the normalized variable u, shows that the reordering of the phase zones of a Fresnel lens according to the Fibonacci sequence produces a symmetrical splitting of the first-order

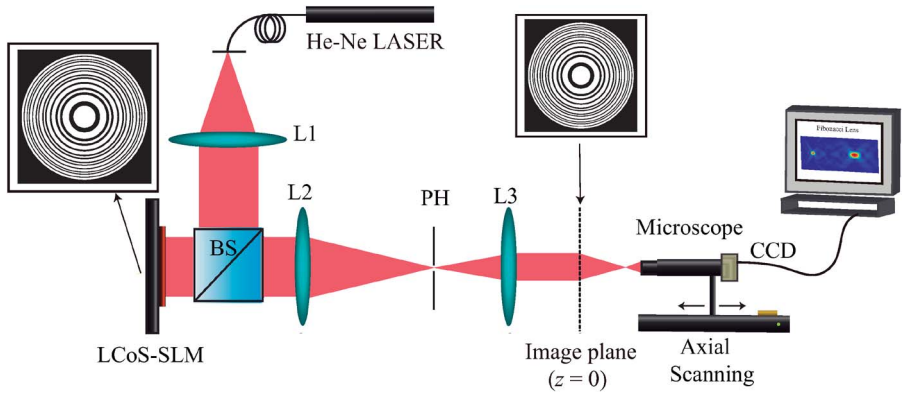

Fig. 3. Experimental setup for the assessment of the focusing properties of FLs. Light source: He-Ne laser $\lambda = 633$ nm. A plane wave-front impinged on the LCoS-SLM (Holoeye PLUTO, with 8-bit gray-level, 8 μm pixel pitch and 1920 $\times$ 1080 pixels) where the lenses are recorded. A microscope objective (10*X* Zeiss© Plan-Apo) is attached to a CCD camera (EO-1312M 1/2″ CCD Monochrome USB Camera, 8-bit gray-level, pixel pitch of 4.65 μm and 1280 $\times$ 1024 pixels). It then performs an axial scanning and records the diffracted field.

focus. Higher diffraction orders also appear due to the binary nature of the structure; therefore, these two foci are periodically replicated along the coordinate u with period F_{j+1} (not shown in Fig. 2). However, only the focal distances associated to first-order foci of the FL are related through the golden mean.

3. Experimental Setup and Its Characterization

For the experimental verification of the singular properties of diffractive lenses with Fibonacci-based structure, we implemented the experimental setup shown in Fig. 3. The proposed lenses were recorded on a Liquid Crystal in a Silicon Spatial Light Modulator (LCoS-SLM), calibrated for a 2π phase shift at $\lambda = 633$ nm (phase-only modulation). In addition to the diffractive lens, a linear phase carrier was modulated on the SLM to avoid noise originating from the specular reflection (zero order of diffraction) and also caused by high diffraction orders due to its pixelated structure. In this way, the addressed signal was guided by the first diffraction order into the focal plane of lens L2 where a pinhole acted as a spatial filter. To compensate the wavefront distortions caused by the lack of flatness of the LCoS-SLM and the other optical components, we first employed a Hartmann–Shack wavefront sensor to measure such wavefront distortions (up to 66 Zernike coefficients) for zero modulation. Then, to compensate the aberrations in the experiment, the complex conjugated of the retrieved phase was added to the other phase components of the lens. The result was addressed to the LCoS-SLM [18].

The focusing properties of FLs were assessed by recording the diffracted field produced when illuminated by a monochromatic plane wave. To correctly sample the diffracted field, we used a motorized stage in which we mounted a microscope objective attached to a CCD camera (EO-1312M 1/2″ CCD Monochrome USB Camera, 8-bit gray-level, pixel pitch of 4.65 μm and 1280 $\times$ 1024 pixels). The experimental result obtained for a S_8 lens with $a = 1.1$ mm is shown in Fig. 4(a). A profile of the measured axial irradiance is depicted in Fig. 4(b), where the theoretical prediction computed numerically using (1) is also represented. As can be seen, both results are in excellent agreement, and the two first-order foci are clearly visible. Although the maximum axial intensity of these foci are equal, the diffraction efficiency of the first focus, i.e., η_1, is higher than second one, i.e., η_2, satisfying $\eta_1/\eta_2 = (u_2/u_1)^2 \approx \varphi^2$. Moreover, the second lobe is φ^2 times broader than the first one, and the transverse width of the second lobe is also φ times greater, so its resolution is lower. As predicted by the theoretical analysis, the axial localization of the focal spots depends on the Fibonacci numbers F_j and F_{j-1}, and such focal distances satisfy the following relationship: $f_1/f_2 = F_j/F_{j-1} \approx \varphi$.

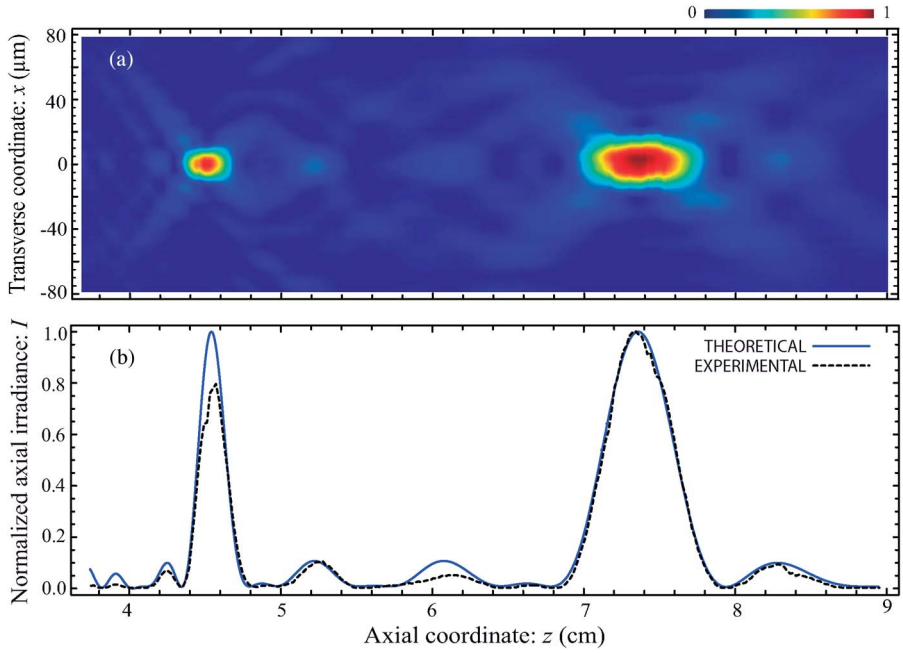

Fig. 4. (a) Evolution of the transverse intensity distribution produced by a zone plate constructed using a Fibonacci structure. Experimental results using a S_8 zone plate (b) Profile of Fig. 4(a) (dotted line) showing the longitudinal irradiance distribution on the optical axis and the relative magnitude of the two foci. The theoretical values of the irradiance are shown in solid line for comparison. In both cases, the values are normalized to the peak intensity. The foci approaches the axial positions $f_1 = a^2/2\lambda F_7 =$ 7.35 cm and $f_2 = a^2/2\lambda F_8 = 4.55$ cm.

4. Conclusion

We have shown that an FL is a lens that naturally produces two foci along the axial coordinate. These foci are located at certain axial positions given by the Fibonacci numbers, being the golden mean the ratio of the two FL focal distances. The foci of a given FL are situated symmetrically, one at each side of the focus of an equivalent Fresnel zone plate of the same number of zones. Moreover, we have found that the golden mean is also the responsible of the energetic balance of both foci and also of its axial and transverse resolution. We believe that new type of diffractive lenses could be of benefit across a broad range of applications where conventional Fresnel zone plates are currently applied, such as X-ray microscopy, THz imaging, and ophthalmology (in the form of bifocal intraocular or contact lenses for the correction of presbyopia). Moreover, as FL can be produced using the same techniques as those used for making Fresnel zone plates, all improvements already reported, such as the resolution increase by double patterning nanofabrication technique [19] or the use of composite zones [20], are still valid for the fabrication of FLs.

References

[1] A. J. Fleming, "Plant mathematics and Fibonacci's flowers," *Nature*, vol. 418, no. 6899, p. 723, Aug. 2002.
[2] G. Linage, F. Montoya, A. Sarmiento, K. Showalter, and P. Parmananda, "Fibonacci order in the period-doubling cascade to chaos," *Phys. Lett. A*, vol. 359, no. 6, pp. 638–639, Dec. 2006.
[3] C. Li, X. Zhang, and Z. Cao, "Triangular and Fibonacci number patterns driven by stress on core/shell microstructures," *Science*, vol. 309, no. 5736, pp. 909–911, Aug. 2005.
[4] R. Coldea, D. A. Tennant, E. M. Wheeler, E. Wawrzynska, D. Prabhakaran, M. Telling, K. Habicht, P. Smeibidl, and K. Kiefer, "Quantum criticality in an Ising chain: Experimental evidence for emergent E8 symmetry," *Science*, vol. 327, no. 5962, pp. 177–180, Jan. 2010.
[5] L. Mahler, A. Tredicucci, F. Beltram, C. Walther, J. Faist, H. E. Beere, D. A. Ritchie, and D. S. Wiersma, "Quasi-periodic distributed feedback laser," *Nat. Photon.*, vol. 4, no. 3, pp. 165–169, Mar. 2010.
[6] R. Dallapiccola, A. Gopinath, F. Stellacci, and L. Dal Negro, "Quasi-periodic distribution of plasmon modes in two-dimensional Fibonacci arrays of metal nanoparticles," *Opt. Exp.*, vol. 16, no. 8, pp. 5544–5555, Apr. 2008.

[7] A. Sakdinawat and Y. Liu, "Soft-X-ray microscopy using spiral zone plates," *Opt. Lett.*, vol. 32, no. 18, pp. 2635–2637, Sep. 2007.
[8] A. Siemion, M. Makowski, J. Suszek, J. Bomba, A. Czerwiski, F. Garet, J.-L. Coutaz, and M. Sypek, "Diffractive paper lens for terahertz optics," *Opt. Lett.*, vol. 37, no. 20, pp. 4320–4322, Oct. 2012.
[9] J. A. Davison and M. J. Simpson, "History and development of the apodized diffractive intraocular lens," *J. Cataract. Refract. Surg.*, vol. 32, no. 5, pp. 849–858, May 2006.
[10] G. Saavedra, W. D. Furlan, and J. A. Monsoriu, "Fractal zone plates," *Opt. Lett.*, vol. 28, no. 12, pp. 971–973, Jun. 2003.
[11] J. A. Davis, S. P. Sigarlaki, J. M. Craven, and M. L. Calvo, "Fourier series analysis of fractal lenses: Theory and experiments with a liquid-crystal display," *Appl. Opt.*, vol. 45, no. 6, pp. 1187–1192, Feb. 2006.
[12] W. D. Furlan, G. Saavedra, and J. A. Monsoriu, "White-light imaging with fractal zone plates," *Opt. Lett.*, vol. 32, no. 15, pp. 2109–2111, Aug. 2007.
[13] J. A. Monsoriu, A. Calatayud, L. Remon, W. D. Furlan, G. Saavedra, and P. Andrés, "Zone plates generated with the Fibonacci sequence," in *Proc. EOS Topical Meet. Diffract. Opt.*, Feb. 2010, pp. 151–152, Preliminary results and the first design of Fibonacci Zone Plates were presented.
[14] E. Maciá, "Exploiting aperiodic designs in nanophotonic devices," *Rep. Prog. Phys.*, vol. 75, no. 3, p. 036502, Mar. 2012.
[15] Y. Sah and G. Ranganath, "Optical diffraction in some Fibonacci structures," *Opt. Commun.*, vol. 114, no. 1/2, pp. 18–24, Jan. 1995.
[16] N. Gao, Y. Zhang, and C. Xie, "Circular Fibonacci gratings," *Appl. Opt.*, vol. 50, no. 31, pp. G142l–G1428, Nov. 2011.
[17] H. T. Dai, Y. J. Liu, and X. W. Sun, "The focusing property of the spiral Fibonacci zone plate," in *Proc. SPIE*, 2012, vol. 8257, p. 82570T.
[18] A. Calatayud, J. A. Rodrigo, L. Remón, W. D. Furlan, G. Cristóbal, and J. A. Monsoriu, "Experimental generation and characterization of devils vortex-lenses," *Appl. Phys. B*, vol. 106, no. 4, pp. 915–919, Mar. 2012.
[19] W. Chao, J. Kim, S. Rekawa, P. Fischer, and E. H. Anderson, "Demonstration of 12 nm resolution Fresnel zone plate lens based soft X-ray microscopy," *Opt. Exp.*, vol. 17, no. 20, pp. 17 669–17 677, Sep. 2009.
[20] L. Kipp, M. Skibowski, R. L. Johnson, R. Berndt, R. Adelung, S. Harm, and R. Seemann, "Sharper images by focusing soft X-rays with photon sieves," *Nature*, vol. 414, no. 6860, pp. 184–188, Nov. 2001.